THE SHAPE OF ENCELADUS FROM A DENSE PHOTOGRAMMETRIC CONTROL NETWORK. M. T. Bland, L. A. Weller, D. P. Mayer, K. L. Edmundson, B. A. Archinal. USGS Astrogeology Science Center, Flagstaff AZ 86001 USA (mbland@usgs.gov).

Summary: We are creating a new shape model for Saturn's moon Enceladus by photogrammetrically solving for latitude, longitude, and radius on a dense network of image tie points. The resulting point cloud is interpolated to a smooth shape model. We are currently assessing how the spatial resolution and vertical accuracy vary across the surface, depending on the image density and stereo strength. When completed, the shape model will be made publicly available, enabling new science, future exploration, and improved spatial data infrastructure (SDI) for Enceladus.

Why Enceladus' shape? Even after the completion of NASA's Cassini mission, Saturn's small moon Enceladus remains an enigma. The moon's ongoing cryovolcanic eruptions, which emanate from hot fractures at the south pole, and the diversity of its surface terrains defy simple explanations. These mysteries, coupled with the potential habitability of its subsurface ocean, have resulted in Enceladus remaining a focus of current investigations and future exploration. Enceladus' shape and topography (here defined as deviation of the shape from the best-fit triaxial ellipsoid) provide fundamental clues to Enceladus' mysteries, including its thermal state [1, 2, 3], internal structure [1, 2, 3], rotational dynamics [4], and tectonic history [5].

Planetary shape information is also one of the three foundational component of "spatial data infrastructure" (SDI) [6, 7], which allows data integration that enables high-quality science and engineering. The work described here also contributes to the two other foundational SDI datasets: geodetic control and rigorously photogrammetrically controlled orthoimages [6].

Previous global shape models of Enceladus have been produced from limb fits [8, 9], including spherical harmonic expansion of limb data to degree 8 [2] and 16 [4] (the latter also includes some photogrammetric tie pointing). Regional or semi-global topography has also been generated from stereo imaging, which provides higher resolution data, but over regionally confined areas (up to 50% of the satellite) [3, 5]. These topographic datasets are of high quality; however, they have their limitations. Those derived from limb data are global in extent but relatively low resolution (degree 16 can resolve features of order 100 km), whereas those derived from stereo data alone are not global. Few of the current shape models, with the notable exception of [4], include a full assessment of the spatial distribution of uncertainties, or are publicly available in easily usable formats (e.g., point clouds).

Shape from photogrammetry: In previous work we used the Integrated Software for Imagers and Spectrometers (ISIS3) [10] to create a global photogrammetric control network and improved image pointing for most of the Enceladus imaging dataset with pixel scale less than 500 m/pixel and phase angle less than 120° [11]. That network consisted of 621 Cassini Imaging Science Subsystem (ISS) narrow and Wide angle camera images, 10,362 tie points and 173,000 measures. The updated pointing kernels resulting from that work facilitated the development of a new, much-denser network (Fig. 1) using the same image set. The new network consists of more than 888,000 tie points (more than a factor of 80 increase) and 30 million measures. We triangulated tie point latitude, longitude, and radius using a least-squares bundle adjustment (*jigsaw* [12]). We then interpolated the point cloud to a smooth shape model using two different approaches: Ames Stereo Pipeline's (ASP) point2dem [13] and ISIS's cnet2dem (Fig. 2). Both methods provide suitable shape models, although preliminary investigations suggest point2dem provides more smoothing and hole-filling versatility.

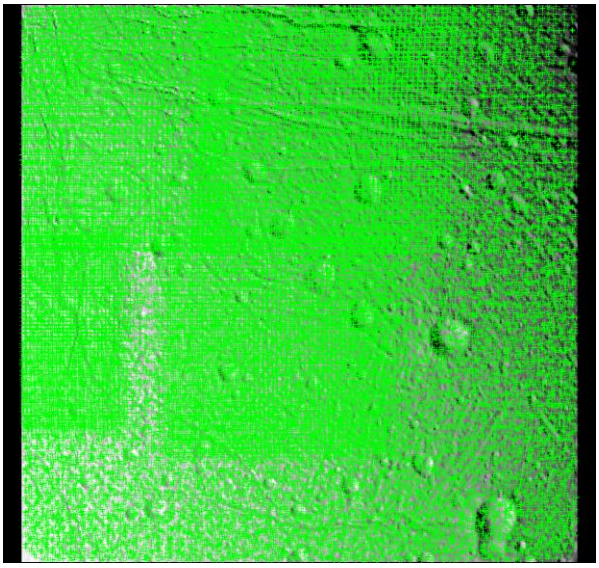

Figure 1: Example of the dense grid of tie points (green dots) utilized in our photogrammetric solution. Tie point density varies with image density. Area shown is 135 km wide by 100 km high.

The preliminary shape model: Figure 2 shows the preliminary shape model produced by interpolating

the point cloud to a scale of 1099 pixels per degree. Enceladus' triaxial shape is evident, with equatorial (*a*, *b*) and polar (*c*) axis of 256.3, 251.2, and 248.3 km, respectively. The triaxial values are within the uncertainty of the IAU values [12]. Several other features are also resolved in the shape model, and are accentuated when the triaxial shape is removed (Fig. 3). The south pole of Enceladus is somewhat flattened, consistent with previous findings [13]. We also see large-scale patterns that are not obviously associated with topography (first identified in [5]), including a set of basins that appears to follow a great circle pattern, similar to that observed in [4]. A more detailed comparison of our shape model with published work is ongoing. Notably, because our shape model has higher spatial resolution (in some regions) than those derived from limb-fits, we can also resolve topography corresponding to actual surface features, including craters in the mid-latitudes, ridges around the south polar terrain, and the prominent dorsa in the trailing hemisphere.

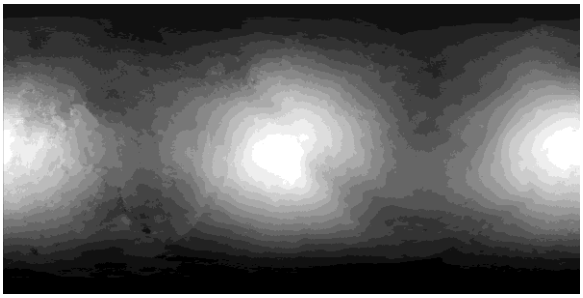

Figure 2: Preliminary global shape model from ISIS' cnet2dem. The triaxial shape is evident (degree-2 pattern). Cylindrical projection, ±90º latitude, 0º-360º longitude. Bright regions are "higher."

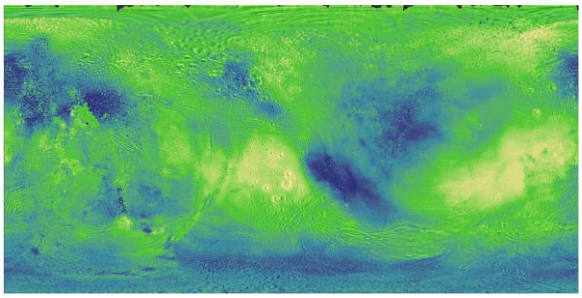

Figure 3: Enceladus "topography" (triaxial shape subtracted) overlain on the ISS basemap. Map projection as in Fig. 2. Blues are low regions and yellows are high. Total relief is ~2 km. In some places individual craters and ridges can be resolved.

Shape model quality assessment: The horizontal "resolution" and vertical accuracy of our model varies spatially. High image density generally corresponds to high tie point density (Fig. 4), and interpolation to smaller pixel scale in those regions is reasonable. In contrast, some regions of Enceladus have sparse coverage, and demand interpolation to larger scales. However, tie point density alone is not an indication of shape model quality. Our method also requires sufficient differences in viewing geometry (i.e., stereo quality) for accurate triangulation of tie points. Where point density and stereo quality are both high, we can resolve craters as small as 7-km in diameter. Where point density and stereo quality is low (e.g., the trailing hemisphere) the shape model is noisy. We are continuing to improve the shape model and will provide quantitative metrics for the spatially variable shape model quality upon its release.

Release to the public: Our shape model is intended as a resource for the planetary science community. Upon completion, the shape model will be released (through the PDS or similar) as both an interpolated product and a point cloud. Our methodology will be documented in a peer-reviewed publication.

Acknowledgements: This effort was supported by the NASA-USGS Interagency Agreement.

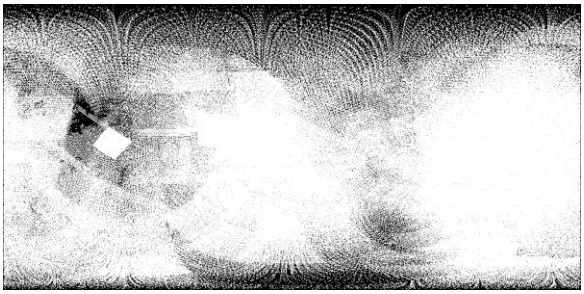

Figure 4: Map of the point density used to interpolate to the shape model. Map projection as in Fig. 2. Point density is highly variable across the surface.

References: [1] Hemingway D. and Mittal, T. (2019). *Icarus* in press. [2] Nimmo, F. et al. (2011) *JGR, 116*, E11001. [3] Giese, B. et al. (2010) *EPSC, 5*, 675. [4] Tajeddine, R. et al. (2017) *Icarus, 295*, 46-60. [5] Schenk, P. and McKinnon, W. (2009) *GRL, 36*, L16202. [6] Laura, J. et al. (2018) *Earth Space Sci., 5*, 486-502. [7] Laura, J. et al. (2017) *ISPRS Int. J. Geo-Inf, 6*, 181. [8] Thomas P. et al. (2007), *Icarus, 190*, 573-584. [9] Thomas, P. (2010) *Icarus, 208*, 395-401. [10] Keszthelyi, L. et al. (2014) *LPSC* 45, #1686. [11] Bland, M. et al. (2018) *Earth Space Sci., 5*, 486-502. [12] Edmundson K. et al. (2012) *ISPRS* I-4, 203-208. [13] Beyer R. et al. (2018) *Earth Space Sci.* 5, 537-548. [14] Archinal, B. et al. (2011). *Celest Mech Dyn Astr* 10.1007/s10569-010-9320-4. [15] Porco C. et al. (2006) *Science* 311, 1393.